An ingestible self-orienting system for oral delivery of macromolecules

HHS Public Access

Author manuscript

Science. Author manuscript; available in PMC 2020 February 08.

Published in final edited form as:

Science. 2019 February 08; 363(6427): 611–615. doi:10.1126/science.aau2277.

An ingestible self-orienting system for oral delivery of macromolecules

Alex Abramson[1], **Ester Caffarel-Salvador**[1,2], **Minsoo Khang**[1], **David Dellal**[2], **David Silverstein**[1], **Yuan Gao**[1], **Morten Revsgaard Frederiksen**[3], **Andreas Vegge**[3], **Frantisek Hubálek**[3], **Jorrit J. Water**[3], **Anders V. Friderichsen**[3], **Johannes Fels**[3], **Rikke Kaae Kirk**[3], **Cody Cleveland**[1,3], **Joy Collins**[1], **Siddartha Tamang**[1], **Alison Hayward**[1,4], **Tomas Landh**[3], **Stephen T. Buckley**[3], **Niclas Roxhed**[1,5], **Ulrik Rahbek**[3], **Robert Langer**[1,2,6,*], and **Giovanni Traverso**[1,7,8,*]

[1]Department of Chemical Engineering and David H. Koch Institute for Integrative Cancer Research, Massachusetts Institute of Technology, Cambridge, MA 02139, USA.

[2]Institute for Medical Engineering and Science, Massachusetts Institute of Technology, Cambridge, MA 02139, USA.

[3]Global Research Technologies, Global Drug Discovery, and Device R&D, Novo Nordisk A/S, Copenhagen, Denmark.

[4]Division of Comparative Medicine, Massachusetts Institute of Technology, Cambridge, MA 02139, USA.

[5]Department of Micro and Nanosystems, KTH Royal Institute of Technology, Stockholm, Sweden.

[6]Media Lab, Massachusetts Institute of Technology, Cambridge, MA 02139, USA.

[7]Department of Mechanical Engineering, Massachusetts Institute of Technology, Cambridge, MA 02139, USA.

[8]Division of Gastroenterology, Brigham and Women's Hospital, Harvard Medical School, Boston, MA 02115, USA.

[*]Corresponding author. rlanger@mit.edu (R.L.); ctraverso@bwh.harvard.edu (G.T.).

Author contributions: A.A., G.T., and R.L. developed the concept, shape, and device. A.A., E.C.-S., M.K., D.D., D.S., Y.G., M.R.F., and N.R. performed tissue characterization. A.A., E.C.-S., D.S., and N.R. conducted millipost studies. A.A., M.K., and M.R.F. developed the actuation system. A.A. and A.V.F. performed Raman spectroscopy. A.A., F.H., and J.J.W. conducted stability studies. A.A., Y.G., A.V., C.C., J.C., S.T., A.H., and N.R. conducted in vivo studies. J.F. developed the AlphaLISA assay. R.K.K. performed histology. A.A., G.T., and R.L. wrote the paper with contributions from T.L., S.T.B., and U.R. All authors discussed results and commented on the manuscript.

Competing interests: M.R.F., A.V., F.H., J.J.W., A.V.F., J.F., R.K.K., C.C., T.L., S.T.B., and U.R. are employees of Novo Nordisk. A.A., E.C.-S., M.K., D.D., Y.G., N.R., R.L., G.T., and M.R.F. are co-inventors on patent applications describing oral biologic drug delivery. R.L. and G.T. report receiving consulting fees from Novo Nordisk. Complete details of all relationships for profit and not for profit for G.T. can be found at www.dropbox.com/sh/szi7vnr4a2ajb56/AABs5N5i0q9AfT1IqIJAE-T5a?dl=0. For a list of entities with which R.L. is involved, compensated or uncompensated, see www.dropbox.com/s/yc3xqb5s8s94v7x/Rev%20Langer%20COI.pdf?dl=0.

Data and materials availability: All data needed to evaluate the conclusions in the paper are present in the paper or in the supplementary materials.

SUPPLEMENTARY MATERIALS

www.sciencemag.org/content/363/6427/611/suppl/DC1

Abstract

Biomacromolecules have transformed our capacity to effectively treat diseases; however, their rapid degradation and poor absorption in the gastrointestinal (GI) tract generally limit their administration to parenteral routes. An oral biologic delivery system must aid in both localization and permeation to achieve systemic drug uptake. Inspired by the leopard tortoise's ability to passively reorient, we developed an ingestible self-orienting millimeter-scale applicator (SOMA) that autonomously positions itself to engage with GI tissue. It then deploys milliposts fabricated from active pharmaceutical ingredients directly through the gastric mucosa while avoiding perforation. We conducted in vivo studies in rats and swine that support the applicator's safety and, using insulin as a model drug, demonstrated that the SOMA delivers active pharmaceutical ingredient plasma levels comparable to those achieved with subcutaneous millipost administration.

Motivated by patient and health care professional preference for oral delivery, research on ingestible biomacromolecule formulations began in 1922, the same year as the first insulin injection (1, 2). This initial study, along with others that followed, was limited by low bioavailability and significant variability. The discovery and purification of insulin transformed our capacity to effectively treat diabetes mellitus (3), yet health care providers delay insulin initiation an average of 7.7 years and instead prescribe less effective oral medications (4). Orally bioavailable biologic dosage forms may allow health care providers to prescribe these effective medications more quickly, yet the development of such systems poses challenges (5). Orally administered therapeutic proteins must navigate extremes of pH, protease-rich environments, thick mucus layers, and cellular tight junctions before achieving systemic bioavailability (6). Preclinical technologies for gastrointestinal (GI)–based biomacromolecule delivery, including permeation enhancers, nanoparticles, and mucusadhering devices, enhance uptake but can generally only safely achieve bioavailabilities on the order of 1% (7–15). Here, we describe a device that physically inserts a drug-loaded millipost through the GI mucosa with the potential of approximating subcutaneous administration bioavailability.

With respect to safety and efficacy, the stomach's 4- to 6-mm-thick wall provides a broader protective layer and more space to insert medication when compared with the 0.1- to 2-mm-thick intestinal walls (16). Additionally, gastric tissue regenerates quickly, and the fluidity of the mucous barrier seals temporary defects in the lining (17, 18). Routine procedures in which gastroenterologists use 5-mm 25-gauge Carr-Locke needles for GI injection provide strong clinical evidence for this action's safety (19, 20). Moreover, by delivering into the stomach tissue rather than the small intestine, the dose delivery time is likely to be more predictable given the recognized variability in gastric emptying (21). Although the idea of delivering biologic drugs to the GI tract via injection has been previously hypothesized and tested via endoscopic procedures (22, 23), here we describe an ingestible self-orienting millimeter-scale applicator (SOMA) that autonomously inserts drug-loaded milliposts into the stomach lining. We demonstrate that the SOMA reliably positions an actuation mechanism to insert active pharmaceutical ingredient (API) into the mucosa rather than the lumen. We also show that the stomach's thick external muscle provides a wide safety margin to prevent perforation during the insertion event. The SOMA's small form factor prevents obstruction in the lower GI tract and allows for easy ingestion. It is smaller in volume than

the U.S. Food and Drug Administration (FDA)-approved daily dosed osmotic-controlled release oral delivery system (OROS) (Ø 9 mm × 15 mm), a nondegradable drug delivery capsule with obstruction rates of 1 in 29 million (24).

Inspired by the self-orienting leopard tortoise (*Stigmochelys pardalis*) (25), we designed a monomonostatic body (26) optimized for rapid selforientation with the capacity to resist external forces (e.g., fluid flow, peristaltic motion, exercise) upon reaching a stable point (Fig. 1). Similar to a weeble-wobble toy, the leopard tortoise has a shifted center of mass and a high-curvature upper shell that enable self-orientation to the preferred upright position. Unlike the weeble-wobble, the tortoise's bottom half possesses a low curvature followed by a corner. Whereas a weeble-wobble can be easily pushed over, the tortoise is stabilized by this shape feature. For the SOMA, we sought a self-orienting shape similar to that of the tortoise to ensure that the millipost would not misfire into the lumen if a patient leaned over during actuation.

Using a custom minimization protocol in MATLAB (see supplementary materials and methods), which applied angular kinematic equations, we designed the SOMA to minimize the mean self-orientation time toward the stomach wall from 36 angles while maximizing the torque required to tilt the device from its preferred orientation. We employed geometric models of tortoise shells as initial guesses for the shape (25). In the model and the final shape, we hollowed out the top of the device to house the actuation mechanism and API milliposts. Selforientation and destabilization testing conducted in vitro with high-speed photography validated our computer model (Fig. 2A and movie S1).

We used a combination of low-density polycaprolactone (PCL) and high-density *316*L stainless steel to produce the low center of mass needed for the SOMA to self-orient. Similarly dense polypropylene and Field's metal were used interchangeably during the in vitro prototyping process. Because stainless steel is not typically ingested, we performed oral acute and subchronic toxicity experiments in rats. No inflammation or signs of toxicity were observed (fig. S1). This is consistent with prior studies, including ones on dental braces (27, 28).

The optimized SOMA shape outperformed both a sphere and ellipsoid made from the same materials with equivalent masses, volumes, and density distributions in two biologically relevant metrics: orientation time and stability. Our simulation predicted that the SOMA oriented most rapidly between the angles of 0° and 45° and the angles of 100° and 180° measured from the preferred orientation, and it oriented within 100 ms from 85% of all initial positions (Fig. 2B). When dropped from a series of random orientations, the simulation predicted that the SOMA possessed the lowest mean orientation time. In vitro studies confirmed that the SOMA oriented most quickly from a 30° and a 135° angle (Fig. 2C).

The device did not orient most rapidly between the angles of 45° and 100° in the simulation or at a 90° angle during in vitro experiments because it possessed a corner in this region. Like the leopard tortoise shell, the corner decreased the applied torque in the stated region but also stabilized the SOMA's preferred orientation. When placed in vitro on a tilt shaker at

50 rpm with excursions of ±15°, the SOMA did not tilt more than a single degree, unlike the ellipsoid and sphere (Fig. 2D). At a 90° starting orientation, all devices were predicted and shown in vitro to orient within the same time frame in water (Fig. 2E). Using this orientation as a control, we tested the effects of fluids with varying viscosities, such as canola oil and gastric juice, on orientation time. The SOMA showed less deceleration due to viscous effects when compared with an ellipsoid.

We tested the SOMA for self-orientation and persistence of mucosal engagement 300 times ex vivo in swine stomachs and 60 times in vivo in fasted swine. To measure proper device orientation, we performed endoscopy on (Fig. 2, F and G) and took x-rays of (fig. S2) the swine after administering the devices through an overtube and agitating the abdomen via 180° rotations and 30° tilts of the animal model. To demonstrate that the mass distribution affected self-orientation, we showed that the SOMA oriented in 100% of trials, whereas a device of the same shape made solely of PCL only oriented 50% of the time.

Having created a localization system, we then fabricated API milliposts. By compressing a mixture of up to 80% human insulin combined with 200,000 molecular weight poly(ethylene) oxide (PEO 200k) under pressures of 550 MPa, we loaded up to 0.5 mg of insulin in a sharp, conical structure measuring 1.7 mm in height and 1.2 mm in diameter. Via compression, we connected the insulin tip to a shaft made solely from biodegradable polymers such as PEO and hydroxypropyl methylcellulose (Fig. 3, A and B). In total, the millipost measured 7 mm in length. Compared with liquid- or solvent-casted formulations, our compressed formulation loaded up to 100 times more API per unit volume (29).

Mechanical and chemical characterization studies on the milliposts supported insulin stability. Raman spectroscopy validated the protein structure of the API after high-pressure exposure (fig. S3 and table S1). Compression tests measured a Young's modulus of 730 ± 30 MPa, like that of PEO, and an ultimate strength of 20.0 ± 0.7 MPa, ensuring millipost integrity after external force (fig. S4). Dissolution profiles in vitro demonstrated complete dissolution within 60 min (fig. S5). Stability studies conducted at 40°C showed that the insulin milliposts remained stable in a desiccated environment for 16 weeks (fig. S6), as compared with 4 weeks of stability for a liquid formulation. Using the same compression concept, we also fabricated millipost tips and shafts out of 100% human insulin, which we used in our SOMA to increase the payload.

Using a custom stage, we demonstrated that milliposts displaced in vivo swine tissue by 7 mm when we applied on the order of 1 N of force (Fig. 3C and fig. S7). Using this measurement as a boundary condition, we created a time-delayed actuation mechanism with forces capable of inserting drug-loaded milliposts into stomach tissue without causing perforation. We used a spring as a power source because of its low space requirement and ability to release energy along one axis almost instantaneously. We loaded the SOMAs with stainless steel springs providing 1.7 to 5 N of force [spring constant (k) = 0.1 to 0.5 N/mm] at full compression. Histology and micro-computed tomography (micro-CT) imaging from in situ and ex vivo experiments demonstrated that milliposts were inserted into the submucosa of swine stomach tissue after being ejected from a SOMA with a 5-N spring. The insulin tips reached the same depth as dye injected by a Carr-Locke needle (Fig. 3, D to

F and H). To ensure a safety margin on the insertion force, we ejected stainless steel milliposts using 9-N steel springs (k = 1.13 N/mm) into ex vivo swine tissue, and these still did not perforate the tissue (Fig. 3, G and I).

To provide a controlled actuation event in the gastric cavity, we required an object with sufficient strength to hold the spring in compression and with predictable brittle fracture mechanics to enable rapid actuation on the millisecond scale. We used sucrose and isomalt to develop a hydration-dependent actuator with these properties. Vents placed in the SOMA allowed GI fluid to dissolve and actuate the barrier. Through COMSOL simulations and in vitro experiments, we demonstrated that sucrose dissolution could be tuned to release a compressed spring at a predicted time with a precision of 11.4 s throughout a 4-min time period (fig. S8).

We administered milliposts loaded with 0.3 mg of human insulin to swine and measured blood glucose and API levels. Endoscopically dosed SOMAs localized to the stomach wall and self-oriented before injecting milliposts into the tissue. Histology confirmed that the SOMA delivered milliposts through the mucosa without injuring the outer muscular layer of the stomach (fig. S9). Subcutaneously dosed milliposts were implanted via manual injection. We also performed a laparotomy followed by a gastrostomy to manually place milliposts into the gastric tissue. These experiments yielded comparable pharmacokinetics and systemic uptake. Milliposts from these experiments released drug at a near zero-order kinetic rate (Fig. 4, A and B). API levels in the swine plasma ranged from 10 to 70 pM throughout the 3.5-hour sampling period. All administration methods yielded a blood glucose–lowering effect (Fig. 4, C and D). We compared these experiments to swine dosed with SOMAs designed to localize the milliposts to the stomach wall without inserting them into the tissue (n = 5). These swine experienced no insulin uptake or blood glucose–lowering effects. Additionally, we showed the potential for sustained-release delivery by subcutaneously implanting milliposts loaded with 1 mg or greater of API. These milliposts released API with a near zero-order rate for at least 30 hours (fig. S10).

A week after dosing the SOMAs, we performed endoscopies and saw no signs of tissue damage or abnormalities from the stomach injections. Veterinary staff monitored the swine twice daily and saw no signs of distress or changes in feeding and stooling patterns after administration. Additionally, to ensure safety in the case of a millipost misfire or device retention, we dosed six SOMA prototypes with 3-mm-long protruding 32-gauge stainless steel needles at once in swine; in this experiment, we performed x-rays over the course of 9 days and found no evidence of GI obstruction, pneumoperitoneum, or other adverse clinical effects (fig. S11). Integrity of the SOMA after GI transit was confirmed by examination of SOMAs recovered after excretion (see supplementary materials and methods). The size and material makeup of the SOMAs are similar to those of FDA-approved ingestible devices such as OROS capsules, ingestible temperature sensors, and capsule endoscopy systems, supporting likely comparable environmental assessments (24, 30, 31).

As tested, the SOMA functioned in vivo only in the fasted state. Animals with food and liquid in their stomachs showed no API uptake when tested with two different SOMAs, but three devices tested in empty stomachs demonstrated successful API delivery (table S2). To

aid in protecting the SOMA from gastric content, we developed a valved membrane insert (fig. S12). As tested in vitro, the valve prevented food particles and viscous liquids from clogging the actuation pathway while still allowing the millipost to pass through.

The SOMA provides a way to deliver insulin orally and could potentially be used to administer other APIs. For example, milliposts fabricated with lysozyme and glucose-6-phosphate dehydrogenase demonstrated full enzymatic activity after undergoing the high-pressure manufacturing process (fig. S13). Of note, the deliverable dose is constrained by the volume, formulation, and stability of the millipost. Increasing the depth and width of millipost penetration will increase drug loading but may compromise the gastric mucosa and increase perforation risk. Further research will be required to determine chronic effects caused by daily gastric injections, foreign body response, and local therapeutic agent exposure. Still, the SOMA represents a platform with the potential to deliver a broad range of biologic drugs, including but not limited to other protein- and nucleic acid-based therapies. The drug delivery efficacy achieved with this technology suggests that this method could supplant subcutaneous injections for insulin and justifies further evaluation for other biomacromolecules.

Supplementary Material

Refer to Web version on PubMed Central for supplementary material.

ACKNOWLEDGMENTS

We thank J. Haupt and M. Jamiel for help with in vivo porcine work; J. Bales and Edgerton Center for high-speed camera use; the MIT Koch Institute Swanson Biotechnology Center histology and imaging cores for technical support; R. Bronson for help with pathology; and U. Stilz, M. Bielecki, T. Kjeldsen, L. F. Iversen, M. O. Jespersen, M. Poulsen, B. Jensen, P. B. Nielsen, J. Trosborg, P. Herskind, C. M. Dalsgaard, and T. B. Pedersen for discussions about SOMA development. We are grateful to all members of the Langer and Traverso laboratories and Novo Nordisk for their biologic drug delivery expertise.

Funding: This work was funded in part by Novo Nordisk grant (R.L., G.T.); NIH grant EB-000244 (R.L., G.T.); NSF GRFP fellowship (A.A.); Division of Gastroenterology, Brigham and Woman's Hospital (G.T.); Viking Olaf Björk scholarship trust (N.R.); and MIT UROP program (M.K., D.D., D.S.).

REFERENCES AND NOTES

1. Fallowfield L et al., Ann. Oncol. 17, 205–210 (2006). [PubMed: 16239231]
2. Harrison GA, BMJ 2, 1204–1205 (1923). [PubMed: 20771392]
3. Diabetes Control and Complications Trial Research Group, N. Engl. J. Med. 329, 977–986 (1993). [PubMed: 8366922]
4. Calvert MJ, McManus RJ, Freemantle N, Br. J. Gen. Pract. 57, 455–460 (2007). [PubMed: 17550670]
5. Caffarel-Salvador E, Abramson A, Langer R, Traverso G, Curr. Opin. Pharmacol. 36, 8–13 (2017). [PubMed: 28779684]
6. Moroz E, Matoori S, Leroux J-C, Adv. Drug Deliv. Rev. 101, 108–121 (2016). [PubMed: 26826437]
7. Aguirre TAS et al., Adv. Drug Deliv. Rev. 106, 223–241 (2016). [PubMed: 26921819]
8. Brayden DJ, Alonso M-J, Adv. Drug Deliv. Rev. 106, 193–195 (2016). [PubMed: 27865345]
9. Prego C, Torres D, Alonso MJ, Expert Opin. Drug Deliv. 2, 843–854 (2005). [PubMed: 16296782]
10. Mathiowitz E et al., Nature 386, 410–414 (1997). [PubMed: 9121559]

11. Banerjee A, Wong J, Gogoi R, Brown T, Mitragotri S, J. Drug Target. 25, 608–615 (2017). [PubMed: 28266884]
12. Koetting MC, Guido JF, Gupta M, Zhang A, Peppas NA, J. Control. Release 221, 18–25 (2016). [PubMed: 26616761]
13. Fox CB et al., ACS Nano 10, 5873–5881 (2016). [PubMed: 27268699]
14. Davies M et al., JAMA 318, 1460–1470 (2017). [PubMed: 29049653]
15. Banerjee A et al., Proc. Natl. Acad. Sci. U.S.A. 115, 7296–7301 (2018). [PubMed: 29941553]
16. Tortora GJ, Derrickson BH, Principles of Anatomy and Physiology (Wiley, ed. 12, 2008).
17. Podolsky DK, J. Gastroenterol. 32, 122–126 (1997). [PubMed: 9058308]
18. Wallace JL, Granger DN, FASEB J. 10, 731–740 (1996). [PubMed: 8635690]
19. Vazharov IP, J. IMAB 18, 273–275 (2012).
20. Eisen GM et al., Gastrointest. Endosc. 55, 784–793 (2002). [PubMed: 12024128]
21. Bolondi L et al., Gastroenterology 89, 752–759 (1985). [PubMed: 3896910]
22. Traverso G et al., J. Pharm. Sci. 104, 362–367 (2015). [PubMed: 25250829]
23. Imran M, Therapeutic agent preparations for delivery into a lumen of the intestinal tract using a swallowable drug delivery device, U.S. Patent 9,844,655 (2017).
24. Bass DM, Prevo M, Waxman DS, Drug Saf. 25, 1021–1033 (2002). [PubMed: 12408733]
25. Domokos G, Várkonyi PL, Proc. Biol. Sci. 275,11–17 (2008). [PubMed: 17939984]
26. Várkonyi PL, Domokos G, Math. Intell. 28, 34–38 (2006).
27. Santonen T, Stockmann-Juvala H, Zitting A, Review on Toxicity of Stainless Steel (Finnish Institute of Occupational Health, 2010).
28. Ortiz AJ, Fernández E, Vicente A, Calvo JL, Ortiz C, Am. J. Orthod. Dentofacial Orthop. 140, e115–e122 (2011). [PubMed: 21889059]
29. Wang M, Hu L, Xu C, Lab Chip 17, 1373–1387 (2017). [PubMed: 28352876]
30. McKenzie JE, Osgood DW, J. Therm. Biol. 29, 605–611 (2004).
31. Iddan G, Meron G, Glukhovsky A, Swain P, Nature 405, 417 (2000).

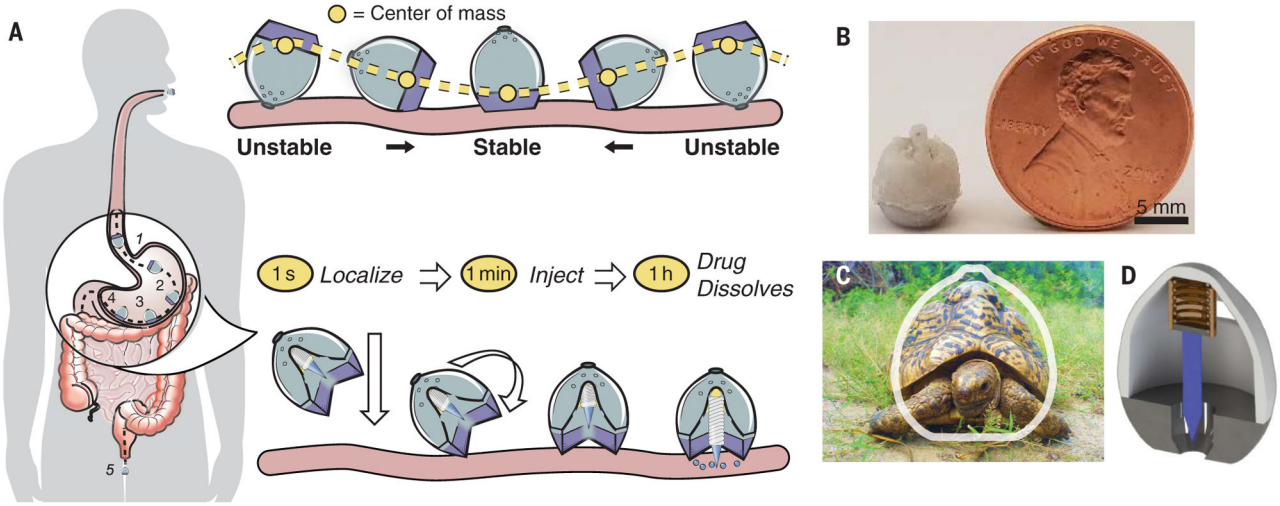

Fig. 1. Mechanical API localization and injection for oral gastric delivery.

(**A**) The SOMA localizes to the stomach lining, orients its injection mechanism toward the tissue wall, and injects a drug payload through the mucosa. The drug dissolves and the rest of the device passes out of the body. (**B**) A fabricated SOMA. (**C**) A comparison between the shape of the leopard tortoise (*S. pardalis*) and that of the SOMA. The SOMA quickly orients and remains stable in the stomach environment after reaching its preferred orientation. [Photo: M. M. Karim/ Wikimedia Commons, CC-BY-SA 2.5] (**D**) The SOMA uses a compressed spring fixed in caramelized sucrose (brown) to provide a force for drug-loaded millipost (blue) insertion. After actuation, the spring remains encapsulated within the device.

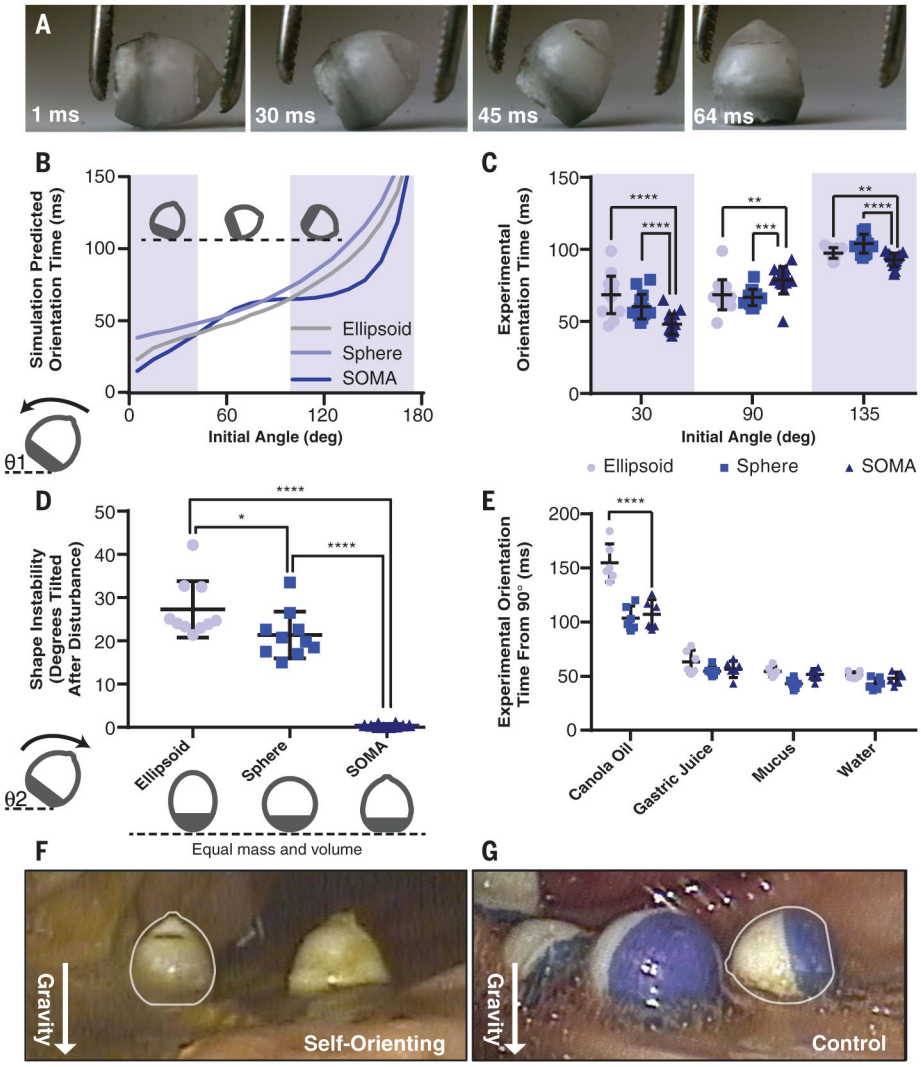

Fig. 2. The SOMA self-orients quickly from any position and remains stable once oriented.

(**A**) Imaging at 1000 frames per second reveals that the SOMA, made from a mixture of PCL and stainless steel, self-orients. (**B**) Simulation-predicted and (**C**) experimentally measured ($n = 15$) orientation times from a given initial angle, θ_1, of ellipsoids, spheres, and SOMAs made from the same mass of PCL and stainless steel. The SOMA self-orients most quickly in the shaded regions between 0° and 45° and between 100° and 180°. The corner on the SOMA lengthens orientation times in the region of 45° to 100°, but (**D**) the corner also stabilizes the preferred orientation. The experimentally determined maximum tilting angle, θ_2, when exposed to a rocking motion of 15° at 0.5 rad/s ($n = 10$), is effectively 0° for the SOMA. This prevents the drug from misfiring into the lumen rather than the tissue. (**E**) Experimentally measured orientation times in fluids with varying viscosities from a 90° starting angle ($n = 6$). (**F**) SOMAs with weighted metal bottoms self-orient in vivo, whereas (**G**) PCL-only SOMAs fail to orient appropriately. Error bars indicate SD. *$P < 0.05$, **$P < 0.01$, ***$P < 0.001$, ****$P < 0.0001$.

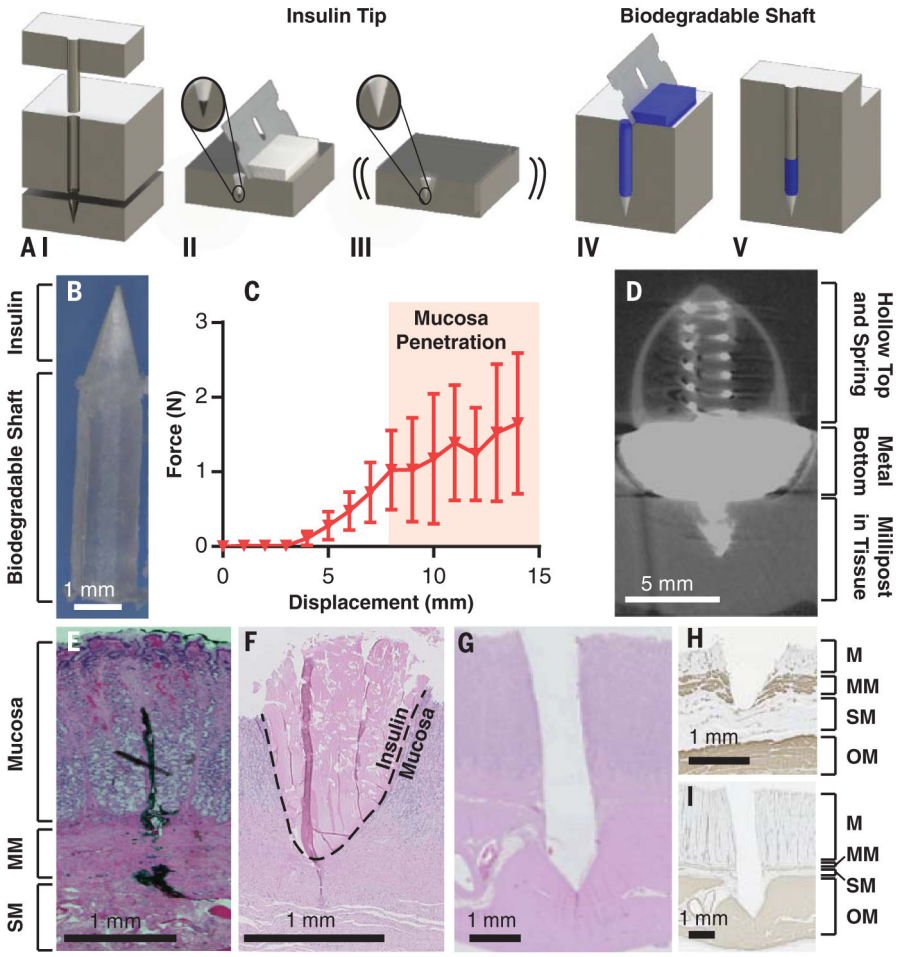

Fig. 3. Millipost fabrication and insertion-force characterization.

(**A**) (I) Millipost stainless steel mold. (II) API mixture screen-printed into tip section. (III) Vibrations ensure powder fills cavity. (IV) Top section filled with biodegradable polymer. (V) Material compressed at 550 MPa. (**B**) 7-mm-long insulin millipost. (**C**) In vivo insertion force profile of insulin milliposts propelled at 0.2 mm/s in swine stomach (n = 2 stomachs, n = 8 insertions). Error bars indicate SD. (**D**) Micro-CT imaging of SOMA delivering a barium sulfate millipost into swine stomach tissue. Bottom is larger to ensure millipost stability during imaging. (**E**) Swine stomach hematoxylin and eosin-stained histology of dye injected by Carr-Locke needle in vivo to demonstrate penetration depth, (**F**) insulin millipost injected via a 5-N spring in the SOMA in situ, and (**G**) steel millipost inserted with a 9-N spring ex vivo. (**H** and **I**) Immunohistochemistry histology stained against α-smooth muscle actin of events in (F) and (G). M, mucosa; MM, muscularis mucosa; SM, submucosa; OM, outer muscularis.

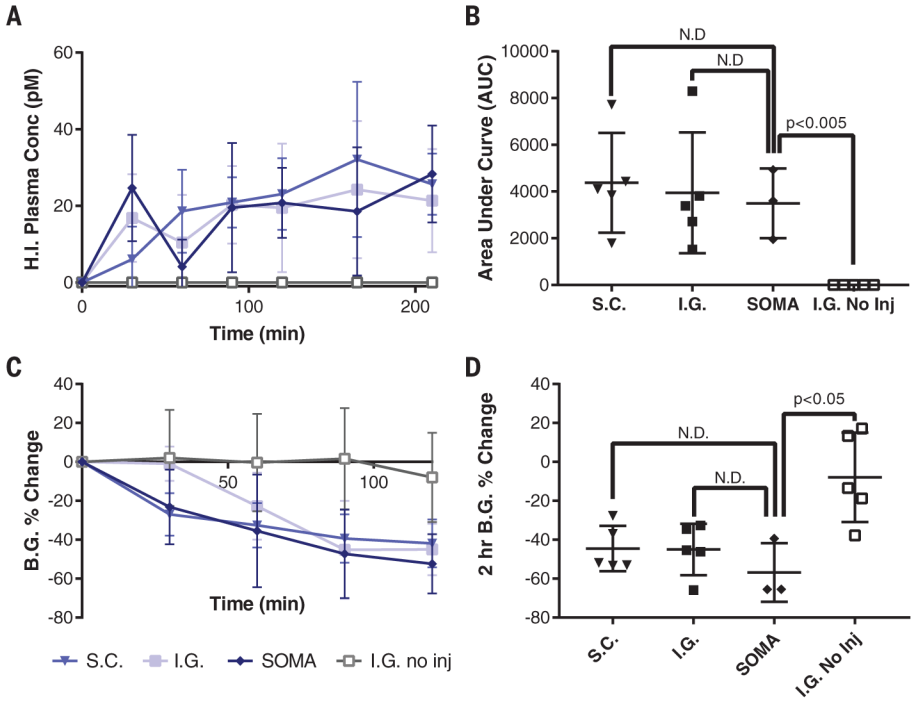

Fig. 4. In vivo API millipost delivery and device evaluation.

(**A** and **B**) Blood plasma levels for human insulin (H.I.) recorded in swine after manual subcutaneous millipost injection (S.C.) ($n = 5$), intragastric (I.G.) surgical millipost placement ($n = 5$), or I.G. millipost placement via a SOMA ($n = 3$). These swine are compared with animals dosed with SOMAs designed to localize the millipost to the tissue wall without injection (I.G. no inj.) ($n = 5$). 300 μg of human insulin was submerged underneath the tissue for each injection trial. Manually placed milliposts contain 80% human insulin and 20% PEO 200k. (**C** and **D**) All swine administered with an insulin injection demonstrated hypoglycemia, and many were rescued with dextrose. The SOMA datasets only include swine with successful fasting without residual food or measurable gastric fluid. Error bars indicate SD. N.D., no statistically significant difference.